Journal of Thermal Analysis and Calorimetry (2022) 147:7865–7873
https://doi.org/10.1007/s10973-021-11065-x

Thermokinetic analysis of the stability of acetic anhydride hydrolysis in isothermal calorimetry techniques

Ye-Cheng Liu[1] · An-Chi Huang[2] · Yan Tang[2] · Chung-Fu Huang[3] · Qing Shen[2] · Chi-Min Shu[4] · Zhi-Xiang Xing[2] · Jun-Cheng Jiang[2]

Received: 31 March 2021 / Accepted: 3 September 2021 / Published online: 26 September 2021

Abstract

Several severe fires and explosions have happened in the past couple of decades. The major cause is addressed to the process reaction initiator. The cumulative heat effect can occur during processing, storage, and transportation. Acetic anhydride, one of the most crucial polymerization initiators, has been investigated in the present paper regarding its high thermal hazard risk. To analyze the thermal stability of acetic anhydride, a reaction calorimeter was used to determine the thermal parameters for stability assessment. We examined acetic anhydride samples under isothermal conditions of 40, 50, and 60 °C and considered factors such as stirring rate, feed rate, and temperature. The findings imply that the optimum operating environment for hydrolysis of acetic anhydride is 50 °C. The Arrhenius equation was used to determine the apparent activation energy of acetic anhydride hydrolysis as 57.77 kJ mol^{-1}. A multiple nonlinear regression model was established to further confirm that the acetic anhydride reaction system was autocatalytic, along with an n-order reaction.

Keywords Process reaction initiator · Cumulative effect of heat · Thermal stability · Reaction calorimeter · Apparent activation energy

Abbreviations

ΔH_a	Heat release range (kJ kg^{-1})
ΔH_b	Heat production rate range [kJ(kg·min)$^{-1}$]
ΔH_d	Heat of decomposition (kJ kg^{-1})
A	Pre-exponential factor (1 s^{-1})
E_a	Apparent activation energy (kJ mol^{-1})
k	Reaction rate constant (dimensionless)
k_0	Reaction rate constant (dimensionless)
q_r	Heat release rate (W)
R	Universal gas constant [8.314 J (mol·K)$^{-1}$]
R^2	Coefficient of determination (dimensionless)
T	Reaction temperature (K)
T_r	Reactor temperature (°C)
T_j	Cooling jacket temperature (°C)
TCL	Conversion limit time (min)
TMR$_{iso}$	Time to maximum rate under isothermal conditions (min

Greek letters

α	Conversion degree (dimensionless)
γ	Conversion rate (dα dt^{-1})

Introduction

The development of the chemical industry has promoted economic growth accompanied by the hazard risk for humans, society, and the environment. According to several severe fire and explosion accidents that have happened in the past couple of decades, the chemical process's danger

---

✉ An-Chi Huang
huangac@cczu.edu.cn

Zhi-Xiang Xing
xingzhixiang@cczu.edu.cn

Jun-Cheng Jiang
jiangjc@cczu.edu.cn

[1] School of Materials Science and Engineering, Changzhou University, No. 21, Gehu mid-Rd., Wujin Dist, Changzhou 213164, Jiangsu, China

[2] School of Environmental and Safety Engineering, Changzhou University, No. 21, Gehu mid-Rd., Wujin Dist, Changzhou 213164, Jiangsu, China

[3] School of Environmental and Chemical Engineering, Zhaoqing University, No. 1, Zhaoqing Blvd, Zhaoqing 526061, Guangdong, China

[4] Department of Safety, Health, and Environmental Engineering, National Yunlin University of Science and Technology, No. 123, University Rd., Sec. 3, Yunlin 64002, Taiwan, ROC

will eventually result in a hazardous accident. The threat of the chemical process is mainly manifested in the thermal runaway reaction. When the heat release rate exceeds the reactor's cooling threshold, the excessive heat accumulation may cause runaway, leakage, explosion, and other consequences. Clarifying the system's thermal safety and carrying out risk analysis are the critical issues of current thermal safety research [1].

Acetic anhydride, which is one of the essential polymerization initiators, plays an important role in chemical synthesis. Because of its superior function and simple reaction process, in the past several decades, acetic anhydride and its hydrolysis have been studied in numerous pieces of literature. In 1984, researchers began to use the hydrolysis of acetic anhydride as a reaction system. Rao first employed acetic hydrolysis as a new reaction system [2], using sulfuric acid to catalyze acetic anhydride hydrolysis in a continuous stirred tank reactor and studying the hydrolysis oscillation characteristics of acetic anhydride. Hydrolysis of acetic anhydride has been used as a benchmark reaction for verifying the new method's correctness in many recent papers [3–5]. Hydrolysis of acetic anhydride was used to rectify the calorimetric reactor's accuracy because of the exothermic of its rapid reaction [6].

Furthermore, acetic anhydride's hydrolysis is a susceptible reaction, worth studying to explore potential applications [7]. Many chemical accidents are continually reminding us of susceptible reaction safety work's importance from the disaster. In 2015, the Tianjin Port fire and explosion accident occurred by neglect of package problems, which is an influential factor leading to the susceptible reaction accident [8]. In 2017, the Arkema chemical plant exploded during Hurricane Harvey in Crosby, Texas, USA. Flooding from the tempest disabled the plant's refrigeration system [9]. Thermal runaway disasters are always unpredictable and often caused by human neglect of intrinsic safety. Therefore, it is necessary to study further and evaluate the essential thermal stability of acetic anhydride hydrolysis.

In this study, we used a reaction calorimeter (RC1) to carry out isothermal experiments and simulated different reaction conditions by controlling the stirring rate, feed rate, and temperature. An isothermal kinetic model was established for linear fitting by analyzing the thermodynamic data of acetic anhydride hydrolysis reaction. The findings of this study could provide a reference for its intrinsic safety and clarify guidance for the use of this reaction in later work.

Experiments and methods

Sample

The main chemicals involved in the experiment included 95–98 mass% sulfuric acid (CAS number: 7664-93-9), acetic anhydride (CAS number: 108-24-7; purity ≥ 98.5%), and deionized water (CAS number: 7732-18-5). Both sulfuric acid and acetic anhydride were purchased from Sinopharm Chemical Reagent Co. (Ningbo, Zhejiang, China).

Reaction of acetic acid hydrolysis

Acetic anhydride, the anhydride of acetic acid, exists in a colorless liquid with a strong odor and strong corrosiveness. Gerhardt first synthesized it in 1852. [10]. The hydrolysis of acetic anhydride is an exothermic reaction which is catalyzed under acidic conditions. The acetic anhydride hydrolysis reaction system is shown in Scheme 1. The hydrolysis reaction system of acetic anhydride is carried out under acidic conditions, and the hydrogen ions and hydroxyl ions ionized by water. The oxygen atom in water attacks the carbonyl carbon to form intermediate 1. Further, the carbon oxygen bond breaks, and the oxygen anion re-forms the carbon oxygen double bond to form intermediate 2 and intermediate 3. One H^+ is removed from intermediate 2 to form an acetic acid molecule, and another H^+ is added to intermediate 3 to form another acetic acid molecule.

The cleavage of carbon–oxygen single bond leads the central carbon to be substituted by nucleophiles; a bimolecular reaction, going further, pertains to a nucleophilic bimolecular solvent substitution reaction. Therefore, the acetic anhydride hydrolysis reaction was inferred to follow the second-order kinetics, and both acetic anhydride and water are first-order kinetics [6]. Given the hydrolysis mechanism of carboxylic acid derivatives, it can be known

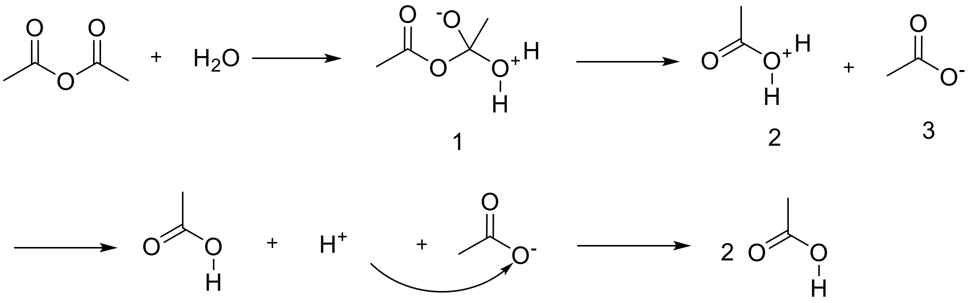

Scheme 1 The acetic anhydride hydrolysis reaction system in sulfuric acid

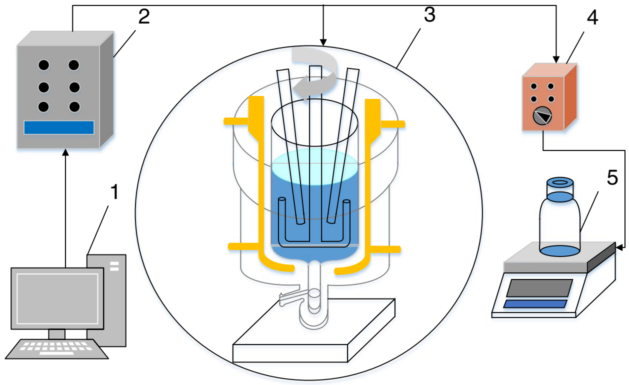

Fig. 1 Reaction calorimeter platform

Table 1 Factors and their corresponding levels

Projects	Factors	Levels		
		1	2	3
A	Temperature/°C	40	50	60
B	Feed Rate/g min^{-1}	5	8	12.5
C	Stirring Rate/rpm	150	200	250

that the hydrolysis of acetic anhydride reaction has a bond break characteristic.

Isothermal experiments by reaction calorimetry (RC1)

The RC1, developed by the Mettler Toledo Co. in Switzerland, is equipped with a low-temperature cooling circulation system, 2 L glass atmospheric pressure reactor, agitator, sensor, and PC host. The reactor temperature (T_r), cooling jacket temperature (T_j), and heat release rate (q_r) can be measured by reaction calorimeter [11, 12], which is presented in Fig. 1. Compared with differential scanning calorimeter, accelerating rate calorimeter, and other thermal analysis techniques, RC1 can dynamically track and monitor the changes of related parameters in the thermal reaction process [13–15].

In this study, RC1 was applied to carry out isothermal experiments, simulate the actual reaction process, and determine a chemical process's thermal risk [16, 17]. The univariate analysis designed the preliminary experiments to ensure the rationality and comprehensiveness of the experimental design. The experimental factors and levels are listed in Table 1. Since the rotating speed upper limit of RC1 under the atmospheric reactor's anchor paddle is 300 rpm, 150, 200, and 250 rpm were set up as our experimental conditions. In the drip speed design, we chose various stirring speeds: 5, 8, and 12.5 g min^{-1}. Under room temperature without catalyst, the hydrolysis reaction of acetic anhydride is relatively slow. However, in the case of catalyst and heating, the hydrolysis speed is intensely accelerated. A certain amount of heat will be released, considering the superposition effect of exothermic and temperature. To delve into the effect of temperature on the exothermic reaction of hydrolysis, we selected temperatures slightly higher than the room temperature for the isothermal experiment: 40, 50, and 60 °C.

The calibration of the equipment was carried out during the installation of the equipment, and the calibration module was set in the iControl software before each group of dropping experiments. Referring to the univariate analysis designed, independent factor experiments were set up to confirm the influence of the system indexes' change of factors. Considering that the volume of RC1 reactor used was 2 L, 1200 g water was used as the bottom liquid to ensure the detector was submerged, 4 g sulfuric acid was used as catalyst, and 50 g acetic anhydride dropwise was also added. In the designed system, the molar ratio of acetic anhydride to sulfuric acid was roughly 12, and that of water to acetic anhydride was ca. 136.

To determine the molar mass of acetic anhydride and sulfuric acid, the mass of the bottom liquid was firstly determined according to the size of the reactor, and the amount of sulfuric acid was verified according to the concentration of the catalyst. Finally, the mass of acetic anhydride was defined according to the exothermic condition obtained from the experiment. The amount of catalyst will affect the reaction [18]. Therefore, the molar mass ratio experiment had sound result feedback. The least amount of catalyst was used to ensure the safety of the laboratory based on the principle.

Results and discussion

Measurement and analysis of thermokinetic parameters

The enthalpy change of the reaction can be obtained by integrating the heat flow change in RC1 experiments. The exothermic enthalpy of the reaction is approximately 28.5 ± 0.5 kJ. It can be seen from Fig. 2 that the reaction principle of RC1 is to adjust the reaction system by controlling the jacket temperature and reactor temperature. It was found that the hydrolysis of acetic anhydride was a detectable exothermic reaction, its steep curve showed that the reaction rate was extremely fast. Once a considerable equivalent system has accumulated heat, the further consequence will inevitably lead to thermal runaway [19].

The hydrolysis state of acetic anhydride under different reaction conditions was studied to explore the intrinsic safety of the acetic anhydride hydrolysis reaction and to further understand the potential factors of heating out of control

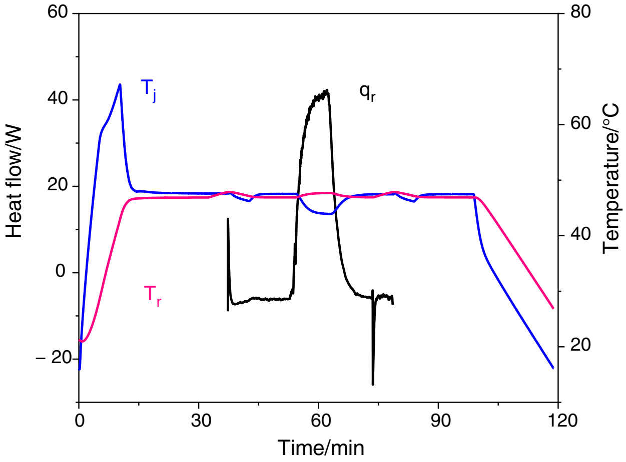

Fig. 2 Temperature and heat flow curves of the reaction process

[20, 21]. Increasing the stirring speed will generally promote the reaction rate, but there is an apparent contradiction in the acetic anhydride hydrolysis system. It can be seen from Fig. 3 (a) and (b) that the promotion effect of high thermal sensitivity coupled with rapid reaction was not obvious under different stirring rates.

An endothermic peak appeared in the curve after the end of the dropping reaction, which was a calibration mechanism of the equipment at the end of the reaction. It can be seen from Fig. 4a that the increase of droplet acceleration speed will accelerate the heat release rate. The acetic anhydride amount added was fixed and the acceleration rate was fast; hence, the exothermic reaction will be completed earlier. Figure 4b diagrams the heat conversion versus time, which further supports the previous conclusion. The curve was steeper in the case of a faster droplet acceleration rate, and the exothermic conversion was completed earlier. These exothermic curves were similar and overlapping because the heat release is independent of the exothermic rate. Figure 5a shows that the temperature has a significant influence on the exothermic reaction system. The initial values of the exothermic peaks all moved forward as temperature increases. When the experiment temperature was 60 °C, the peak value of exothermic heat flux was in a state of continuous fluctuation. Compared with the case of 40 and 50 °C, the integral value was obviously increased, that is the heat release of reaction slightly increased as temperature rises. Figure 5b presents that the exothermic reaction will accelerate with the increase of temperature in the early stage of the reaction, which is also consistent with Fig. 5a.

Fig. 3 Heat flow variation (**a**) and thermal conversion (**b**) at different stirring rate

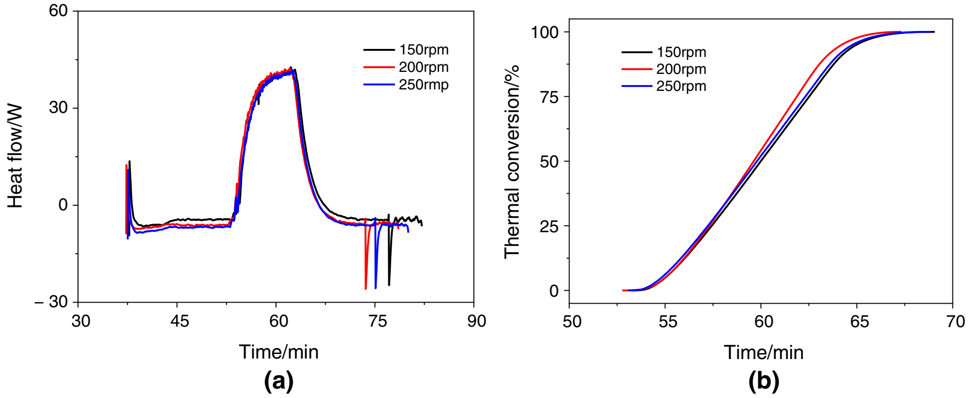

Fig. 4 Heat flow variation (**a**) and thermal conversion (**b**) at different feed rate

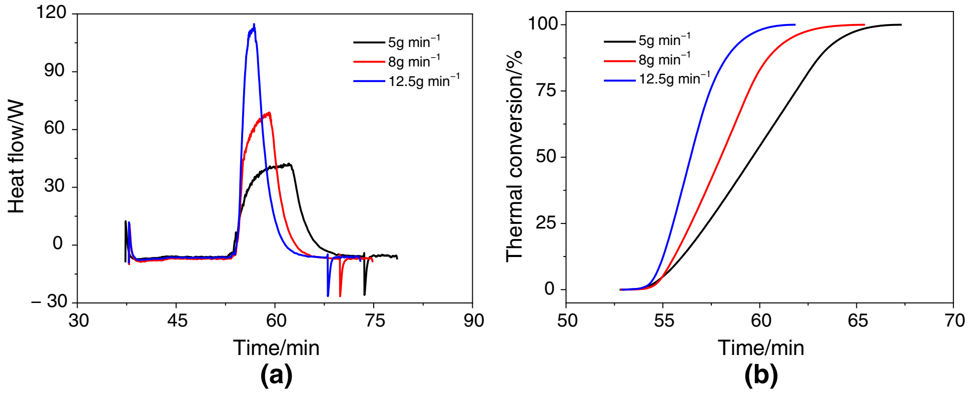

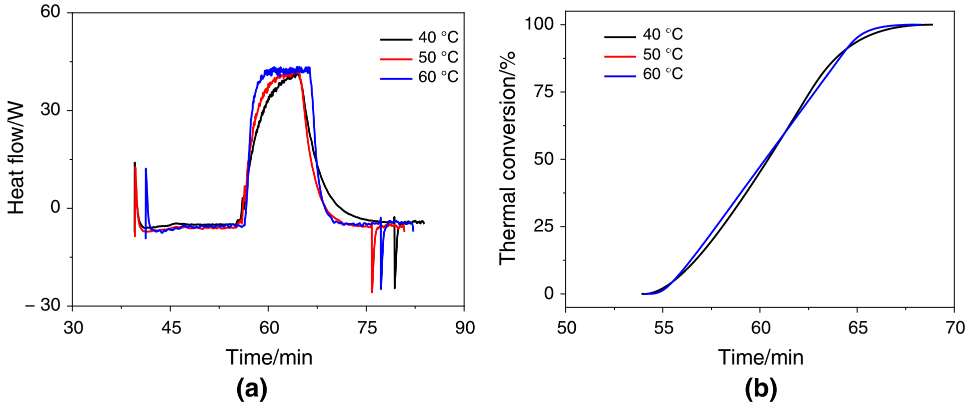

Fig. 5 Heat flow variation (**a**) and thermal conversion (**b**) at different temperature

Table 2 The values of parameters of Arrhenius model

T/K	T^{-1}/–	*k*/–	ln*k*/–
313.15	0.003193	3. 68,701	1.304816
318.15	0.003143	4.67181	1.541568
323.15	0.003095	6.78076	1.914089
328.15	0.003047	10.0216	2.304743
333.15	0.003002	13.2625	2.584941

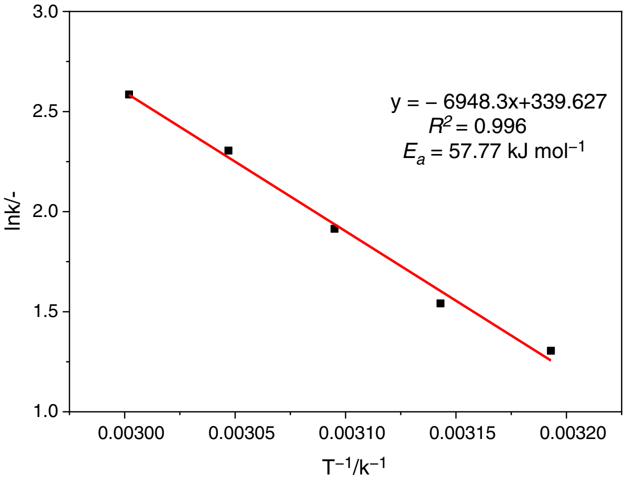

Fig. 6 Isothermal Arrhenius kinetic model

Kinetics model of acetic anhydride hydrolysis

An isothermal kinetic model was used to determine the thermodynamic parameters. According to the Arrhenius equation, various dynamic models were derived, as shown in Eqs. (1) and (2) [22, 23].

$$k = A\exp(-\frac{E_a}{RT}) \tag{1}$$

The following Eq. (2) can be obtained by indefinite integration on both sides of Eq. (1).

$$\ln k = \ln A - \frac{E_a}{RT} \tag{2}$$

where k is the reaction rate constant; A is the pre-exponential factor; E_a is the apparent activation energy, kJ mol^{-1}; R is the universal gas constant, 8.314 J mol^{-1}·K^{-1}; T is the reaction temperature, K.

The Arrhenius equation was used and we further adopted the linear regression method to fit the thermokinetic data obtained from RC1 isothermal experiments. The parameters are showcased in Table 2, and the fitting graph is delineated in Fig. 6. The reaction system's E_a was determined as 57.77 kJ mol^{-1}, which was similar to that obtained by different methods under the similar acetic anhydride concentration in the literature [24].

Practically speaking, most chemical reactions are complex processes, usually consisting of independent, parallel, and continuous stages [25]. To further confirm the stage and reaction order of the reaction system, a multiple nonlinear regression model was used to fit the heat flow curve and to estimate various kinetic parameters [26–29].

Compared with similar experiments carried out, the hydrolysis of acetic anhydride in excess water was assumed as a pseudo-first-order reaction [6]. The findings of this study reveal similar incompleted results with the literature. The E_a was 58.62 kJ mol^{-1}, consistent with the calculated value by the Arrhenius equation [30]. The hydrolysis reaction of acetic anhydride was the first-order reaction of water and anhydride. Under the catalysis of solid acid, the apparent rate reached the second-order and increased linearly with the increase of the concentration of solid acid [2, 31].

In order to further clarify the micro-situation of the acetic anhydride hydrolysis reaction, the hydrolysis kinetics of acetic anhydride was determined by multiple nonlinear regression. Nevertheless, the results showed that the exothermic reaction of acetic anhydride hydrolysis was complicated, not a single first-order reaction as generally assumed, but with multiple stages.

The hydrolysis of acetic anhydride was supposed to include two stages. Here we used A to B1 and B1 to B to represent the two stages of the reaction. B1 referred to a transition step during the reaction. The A to B1 stage was simulated using autocatalytic reaction, as expressed in Eqs. (3) and (4) [32, 33].

$$\frac{\mathrm{d}\alpha}{\mathrm{d}t} = k_0 \mathrm{e}^{-\frac{\mathrm{E_a}}{\mathrm{RT}}} f(\alpha) \tag{3}$$

$$\frac{\mathrm{d}\alpha}{\mathrm{d}t} = k_0 \mathrm{e}^{-\frac{\mathrm{E_a}}{\mathrm{RT}}} (1-\alpha)^{\mathrm{n1}} (z+\alpha)^{\mathrm{n2}} \tag{4}$$

The n-order reaction was used to simulate B1 to B, as illustrated in Eqs. (5) and (6).

$$\frac{\mathrm{d}\alpha}{\mathrm{d}t} = k_0 \mathrm{e}^{-\frac{\mathrm{E_a}}{\mathrm{RT}}} (1-\alpha) \tag{5}$$

$$\frac{\mathrm{d}\gamma}{\mathrm{d}t} = k_0 \mathrm{e}^{\frac{-\mathrm{E}}{\mathrm{RT}}} (\alpha-\gamma)^{\mathrm{n}} \tag{6}$$

where γ is the degree conversion of ratio.

The simulation results show that two parts of the hydrolysis reaction system were composed of the n-order reaction followed by an autocatalytic reaction, as illustrated in Fig. 7. The beginning of the acetic anhydride hydrolysis reaction was a stage of autocatalytic reaction, then n-order and autocatalytic reactions took place simultaneously. Finally, the autocatalytic reaction ended first, and the single n-order reaction maintained the exothermic reaction.

According to the simulation results by multiple nonlinear regression methods, we speculated that the autocatalytic reaction in the previous stage was an indispensable part of acetic anhydride's hydrolysis reaction, although its heat release was small. Assuming that there was no autocatalytic stage, we also performed the corresponding simulation calculation. However, the single n-order reaction simulation results, inconsistent with the actual thermodynamic model, cannot fit the kinetic model from the experiments perfectly. Therefore, the hydrolysis of acetic anhydride was speculated as a multi-step reaction involving autocatalytic and n-order reaction.

As listed in Table 3, the autocatalytic and n-order model simulation results of acetic anhydride hydrolysis kinetics were analyzed, compared, and elucidated. The results showed that the E_a, A, and decomposition heat of acetic anhydride hydrolysis increased in the A to B1 stage (autocatalytic), following the temperature increase. Furthermore,

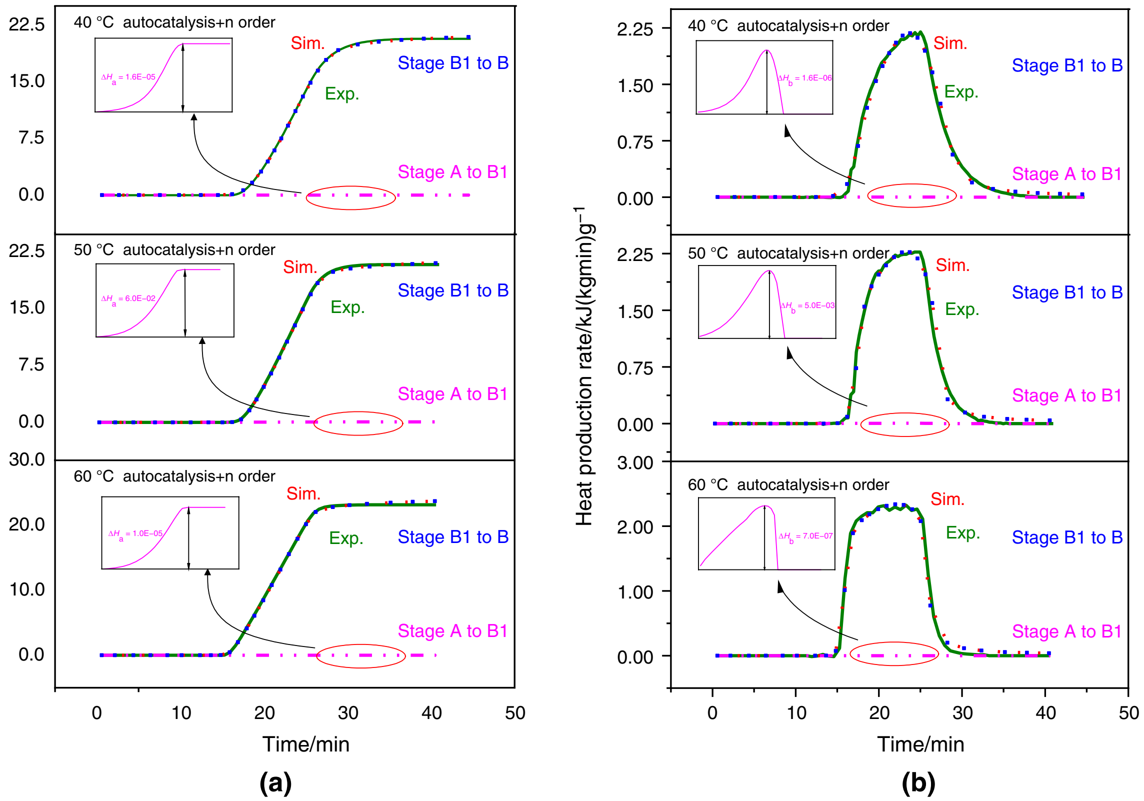

Fig. 7 Simulations and experiments of heat production and heat production rate vs. time for acetic anhydride hydrolysis system under autocatalysis, n-order, and multiple stage reaction models fitting of 40, 50, and 60 °C

Table 3 Reaction kinetic simulation for acetic anhydride hydrolysis system using autocatalysis and n-order models

	Autocatalysis A to B1			n-order B1 to B		
Temperature/°C	40	50	60	40	50	60
ln A/ln s^{-1}	6.2958	7.4636	20.3615	15.8353	46.9876	23.8862
E_a/kJ mol^{-1}	30.9983	36.0263	73.6646	31.5600	100.4784	42.2011
Reaction order n1	0.4949	0.2759	0.2412	8.1751	15.7062	14.9862
Reaction order n2	1.0636	0.8162	0.7194	–	–	–
ΔH_d/kJ kg^{-1}	1.618E-05	0.0598	1.000E-05	25.3372	29.2063	33.0252

– Not applicable

during the B1 to B n-order stage, the decomposition heat increased in the wake of temperature rise. It means that the increase of temperature promotes the autocatalytic reaction of the system within a specific temperature range.

In line with the multiple nonlinear regression fitting results, we also noticed that E_a of the acetic anhydride hydrolysis system was higher at 50 °C than that of 40 and 60 °C. The higher E_a at 50 °C indicated that the thermal stability is more suitable for the experimental platform.

TMR_{iso} is the time for the reaction to reach the maximum reaction rate under isothermal conditions [34, 35]. TCL represents the time required to reach the specified conversion limit [36]. In addition, the isothermal experiment's thermal parameters at 50 °C were utilized to illustrate the safety diagram about TMR_{iso} and TCL. Figure 8 shows the maximum rate time (TMR_{iso}) and conversion limit time (TCL) of acetic anhydride hydrolysis using the autocatalytic, along with n-order reaction models in RC1 isothermal experiment. The results revealed the conversion rate would reach the limit value (10%) at ordinary temperature for about 30 min. The acetic anhydride has shallow stability in the acidic water system, and the consumption of acetic anhydride will occur in a very short time if it is not handled properly. Simultaneously, the TMR_{iso} curve showed that the hydrolysis reaction rate was exceptionally very fast, and the value of TMR_{iso} at room temperature was relatively small, which was ca. 60 min, as depicted in Fig. 8.

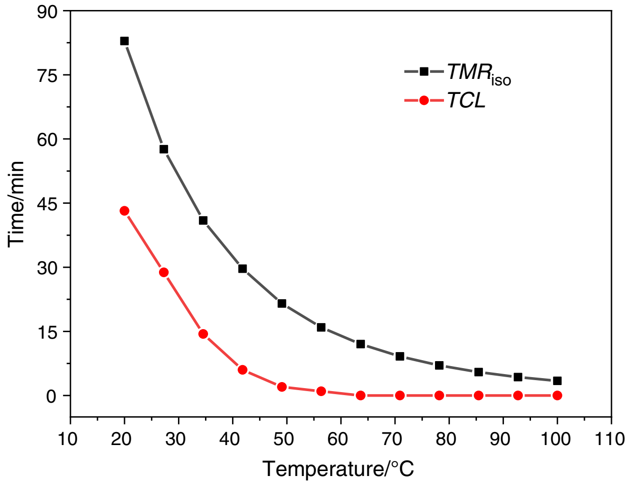

Fig. 8 TCL and TMR_{iso} of acetic anhydride hydrolysis system

Conclusions

The acetic anhydride hydrolysis reaction is a kind of slight and rapid exothermic reaction. However, in the actual chemical process production and storage, acetic anhydride is always used in a large amount. In the case of poor heat dissipation, heat accumulation is greater than heat loss, or if the cooling system fails, it may lead to a runaway reaction, causing combustion and explosion accidents. For this reason, through the RC1 experiment to reduce the actual production and storage process, explore the acetic anhydride hydrolysis system, the conclusions are as follows:

1. The E_a value calculated by this acetic anhydride experimental system using the Arrhenius equation was 57.77 kJ mol^{-1}, similar to the traditionally recognized hydrolysis value of acetic anhydride could give a good performance [30].
2. According to the multiple nonlinear regression model of acetic anhydride hydrolysis, it was found that the first-order reaction of acetic anhydride hydrolysis with excess water may include a tiny part of an autocatalytic reaction, along with n-order reaction [26].
3. On the basis of the safety parameters about TCL (10%) and TMR_{iso}, it could be found that the conversion time of this reaction was extremely fast compared with other reactions, which was a prompt exothermic reaction [37].
4. The acetic anhydride hydrolysis experiment, under the effects of temperature (30, 40, and 50 °C), drop acceleration (5, 8, and 12.5 g min^{-1}), and rotational speed (150, 200, and 250 rpm), could be used in laboratory equipment courses, and the operating parameters under all the conditions were set up expressly.
5. The actual situation of acetic anhydride storage and transport in commercial-scale storage tanks still need to be further explored to provide the reference significance for practical applications.

Acknowledgements The authors thank the National Nature Science Foundation of China (No. 21927815), the National Key Research Development Program of China (No. 2019YFC0810701), Jiangsu Province Postgraduate Research and Practice Innovation Project (KYCX21_2802), and General Natural Science Research Project of Jiangsu Universities in 2020 (No. 20KJB620002) for financial support.

References

1. Tsai YT, Huang GT, Zhao JQ, Shu CM. Dust cloud explosion characteristics and mechanisms in MgH2-based hydrogen storage materials. AlChE J. 2021. https://doi.org/10.1002/aic.17302.
2. Garcia JM, R.B. Bernardino I, Calasans V, Giudici R. . Kinetics of the hydrolysis of acetic anhydride using reaction calorimetry: effects of strong acid catalyst and salts. Chem Eng Res Des. 2021;166:29–39.
3. Garcia Hernandez EA, Souza CR, Vernières Hassimi L, Leveneur S. Kinetic modeling using temperature as an on-line measurement: application to the hydrolysis of acetic anhydride, a revisited kinetic model. Thermochim Acta. 2019;682:178409.
4. Ładosz A, Kuhnle C, Jensen KF. Characterization of reaction enthalpy and kinetics in a microscale flow platform. React Chem Eng. 2020;5:2115–22.
5. Jayakumar NS, Thomas M, Sahu JN. Experimental and modeling of a non-isothermal CSTR to find out parameter regions and conditions causing input multiplicity for acid catalyzed hydrolysis of acetic anhydride. Chemom Intell Lab Syst. 2014;135:213–22.
6. Hirota WH, Rodrigues RB, Sayer C, Giudici R. Hydrolysis of acetic anhydride: non-adiabatic calorimetric determination of kinetics and heat exchange. Chem Eng Sci. 2010;65:3849–58.
7. Gómez García MÁ, Dobrosz Gómez I, Ojeda Toro JC. Thermal stability and dynamic analysis of the acetic anhydride hydrolysis reaction. Chem Eng Sci. 2016;142:269–76.
8. Chen Q, Wood M, Zhao J. Case study of the Tianjin accident: Application of barrier and systems analysis to understand challenges to industry loss prevention in emerging economies. Process Saf Environ Prot. 2019;131:178–88.
9. Wood MH, Fabbri L. Challenges and opportunities for assessing global progress in reducing chemical accident risks. Prog Disaster Sci. 2019;4:100044.
10. Ponnuchamy V. A theoretical investigation of different point charges combined with GAFF and OPLS-AA for acetic anhydride. Chem Phys Lett. 2020;754:137707.
11. Wang Z, Cao DL, Xu ZS, Wang JL, Chen LZ. Thermal safety study on the synthesis of HMX by nitrourea method. Process Saf Environ Prot. 2020;137:282–8.
12. Guo ZC, Chen LP, Rao GN, Chen WH. Kinetic-parameters-free determination of thermally safe operation conditions for isoperibolic homogeneous semibatch reactions: a practical procedure. Chem Eng J. 2017;326:489–96.
13. Sun Y, Ni L, Papadaki M, Jiao Z, Zhu W, Jiang J, et al. Reaction hazard and mechanism study of H_2O_2 oxidation of 2-butanol to methyl ethyl ketone using DSC, Phi-TEC II and GC-MS. J Loss Prev Process Ind. 2020;66:104177.
14. Sun Y, Ni L, Papadaki M, Zhu W, Jiang J, Mashuga C, et al. Process hazard evaluation for catalytic oxidation of 2-octanol with hydrogen peroxide using calorimetry techniques. Chem Eng J. 2019;378:122018.
15. Zhao C, Sun J, Wang Q. Thermal runaway hazards investigation on 18650 lithium-ion battery using extended volume accelerating rate calorimeter. J Energy Storage. 2020;28:101232.
16. Huang AC, Li ZP, Liu YC, Tang Y, Huang CF, Shu CM, et al. Essential hazard and process safety assessment of para-toluene sulfonic acid through calorimetry and advanced thermokinetics. J Loss Prev Process Ind. 2021;72:104558.
17. Zhou J, Yu A-D, Suetor CG, Liang X-M, Hua M, Pan X-H, et al. Risk assessment of polyarylether polymerization process. J Therm Anal Calorim. 2020;144:295–303.
18. Yuan C, Chen W, Yang Z, Huang Z, Yu X. The effect of various cations/anions for MgH_2 hydrolysis reaction. J Mater Sci Technol. 2021;73:186–92.
19. Sahu JN, Mahalik KK, Patwardhan AV, Meikap BC. Equilibrium studies on hydrolysis of urea in a semi-batch reactor for production of ammonia to reduce hazardous pollutants from flue gases. J Hazard Mater. 2009;164:659–64.
20. Sahu JN, Hussain S, Meikap BC. Computational fluid dynamics modeling for urea hydrolysis in a batch reactor for flue gas conditioning. Chem Eng Technol. 2011;34:1347–52.
21. Mahalik K, Sahu JN, Patwardhan AV, Meikap BC. Statistical modelling and optimization of hydrolysis of urea to generate ammonia for flue gas conditioning. J Hazard Mater. 2010;182:603–10.
22. Huang AC, Huang CF, Tang Y, Xing ZX, Jiang JC. Evaluation of multiple reactions in dilute benzoyl peroxide concentrations with additives using calorimetric technology. J Loss Prev Process Ind. 2021;69:104373.
23. Huang AC, Liao FC, Huang CF, Tang Y, Zhang Y, Shu CM, et al. Calorimetric approach to establishing thermokinetics for cosmeceutical benzoyl peroxides containing metal ions. J Therm Anal Calorim. 2021;144:373–82.
24. Shatynski JJ, Hanesian D. Adiabatic kinetic studies of the cytidine/acetic anhydride reaction by utilizing temperature versus time data. Ind Eng Chem Res. 1993;32:594–9.
25. Tseng JM, Lin CP. Prediction of incompatible reaction of dibenzoyl peroxide by isothermal calorimetry analysis and green thermal analysis technology. J Therm Anal Calorim. 2011;107:927–33.
26. Huang AC, Huang CF, Xing ZX, Jiang JC, Shu CM. Thermal hazard assessment of the thermal stability of acne cosmeceutical therapy using advanced calorimetry technology. Process Saf Environ Prot. 2019;131:197–204.
27. Liu SH, Cao CR, Lin WC, Shu CM. Experimental and numerical simulation study of the thermal hazards of four azo compounds. J Hazard Mater. 2019;365:164–77.
28. Cao CR, Liu SH, Das M, Shu CM. Evaluation for the thermokinetics of the autocatalytic reaction of cumene hydroperoxide mixed with phenol through isothermal approaches and simulations. Process Saf Environ Prot. 2018;117:426–38.
29. Chen WC, Lin JR, Liao MS, Wang YW, Shu CM. Green approach to evaluating the thermal hazard reaction of peracetic acid through various kinetic methods. J Therm Anal Calorim. 2016;127:1019–26.
30. Gómez García MÁ, Dobrosz-Gómez I, Ojeda Toro JC. Thermal stability and dynamic analysis of the acetic anhydride hydrolysis reaction. Chem Eng Sci. 2016;142:269–76.
31. Yang YP, Huang AC, Tang Y, Liu YC, Wu ZH, Zhou HL, et al. Thermal stability analysis of lithium-ion battery electrolytes based on lithium bis(trifluoromethanesulfonyl)imide-lithium difluoro(oxalato)borate dual-salt. Polymers (Basel). 2021;13:707.
32. Tsai YT, Yang Y, Huang HC, Shu CM. Inhibitory effects of three chemical dust suppressants on nitrocellulose dust cloud explosion. AIChE Journal. 2020. https://doi.org/10.1002/aic.16888.
33. El Hazzat M, Sifou A, Arsalane S, El Hamidi A. Novel approach to thermal degradation kinetics of gypsum: application of peak deconvolution and Model-Free isoconversional method. J Therm Anal Calorim. 2019;140:657–71.
34. Huang AC, Chen WC, Huang CF, Zhao JY, Deng J, Shu CM. Thermal stability simulations of 1,1-bis(tert-butylperoxy)-3,3,5 trimethylcyclohexane mixed with metal ions. J Therm Anal Calorim. 2017;130:949–57.

35. Wang Q, Liu SH, Huang AC, Huang CF, Chuang YK, Shu CM. Effects of mixing malic acid and salicylic acid with metal oxides in medium- to low-temperature isothermal conditions, as determined using the thermal activity monitor IV. J Therm Anal Calorim. 2018;133:779–84.
36. Cheng YF, Liu SH, Shu CM, Zhang B, Li YF. Energy estimation and modeling solid thermal explosion containment on reactor for three organic peroxides by calorimetric technique. J Therm Anal Calorim. 2017;130:1201–11.
37. Cao CR, Liu SH, Shu CM. Reaction simulation of multistage evaluations for AMBN based on DSC experiments. Thermochim Acta. 2018;661:18–26.